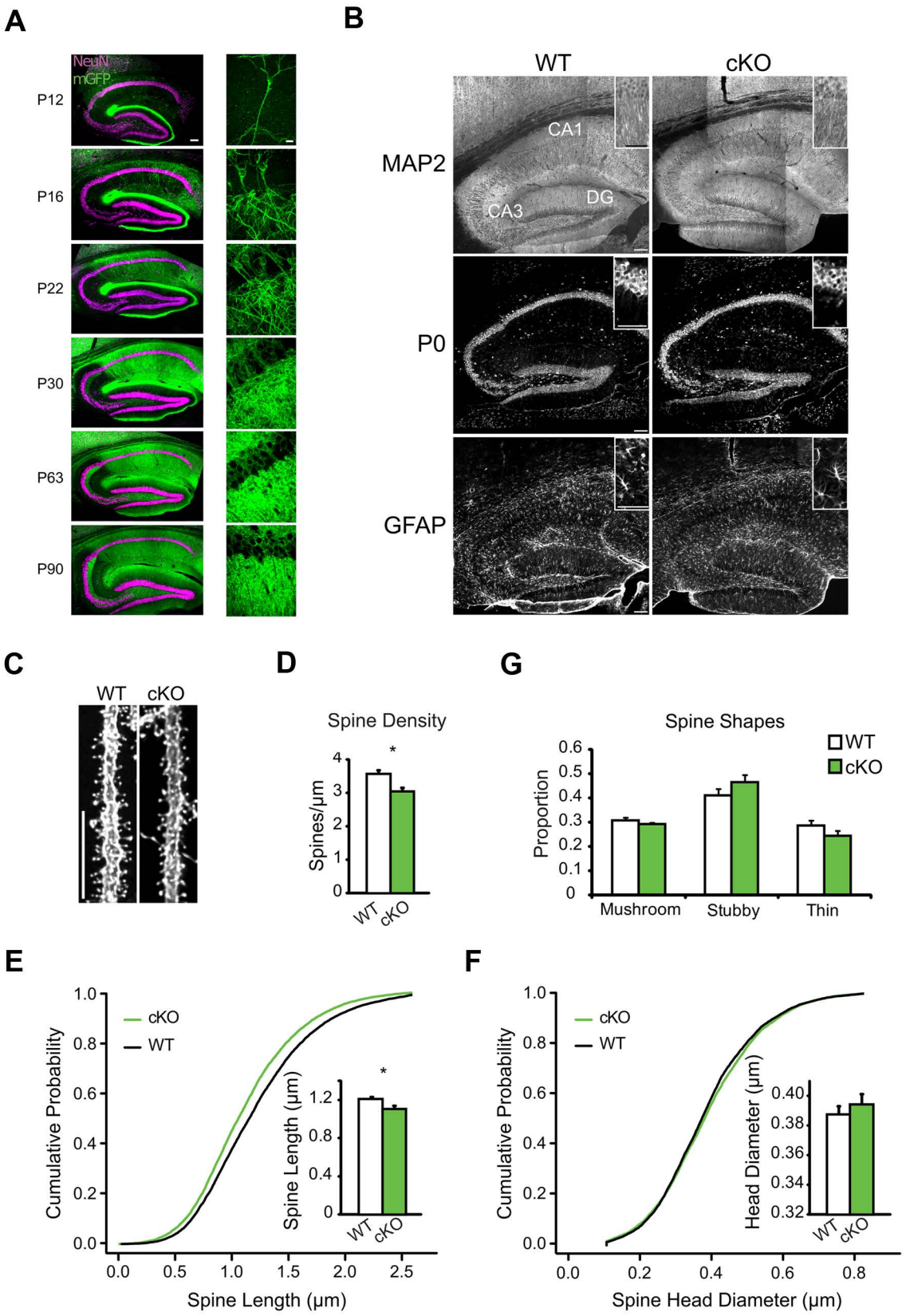
A
NeuN
mGFP
P12
P16
P22
P30
P63
P90
B
WT
cKO
MAP2
P0
GFAP
CA1
CA3
DG
C
WT
cKO
D
Spine Density
Spines/µm
WT
cKO
G
Spine Shapes
WT
cKO
Proportion
Mushroom
Stubby
Thin
E
cKO
WT
Cumulative Probability
Spine Length (µm)
F
cKO
WT
Cumulative Probability
Head Diameter (µm)
Spine Head Diameter (µm)

Figure S1

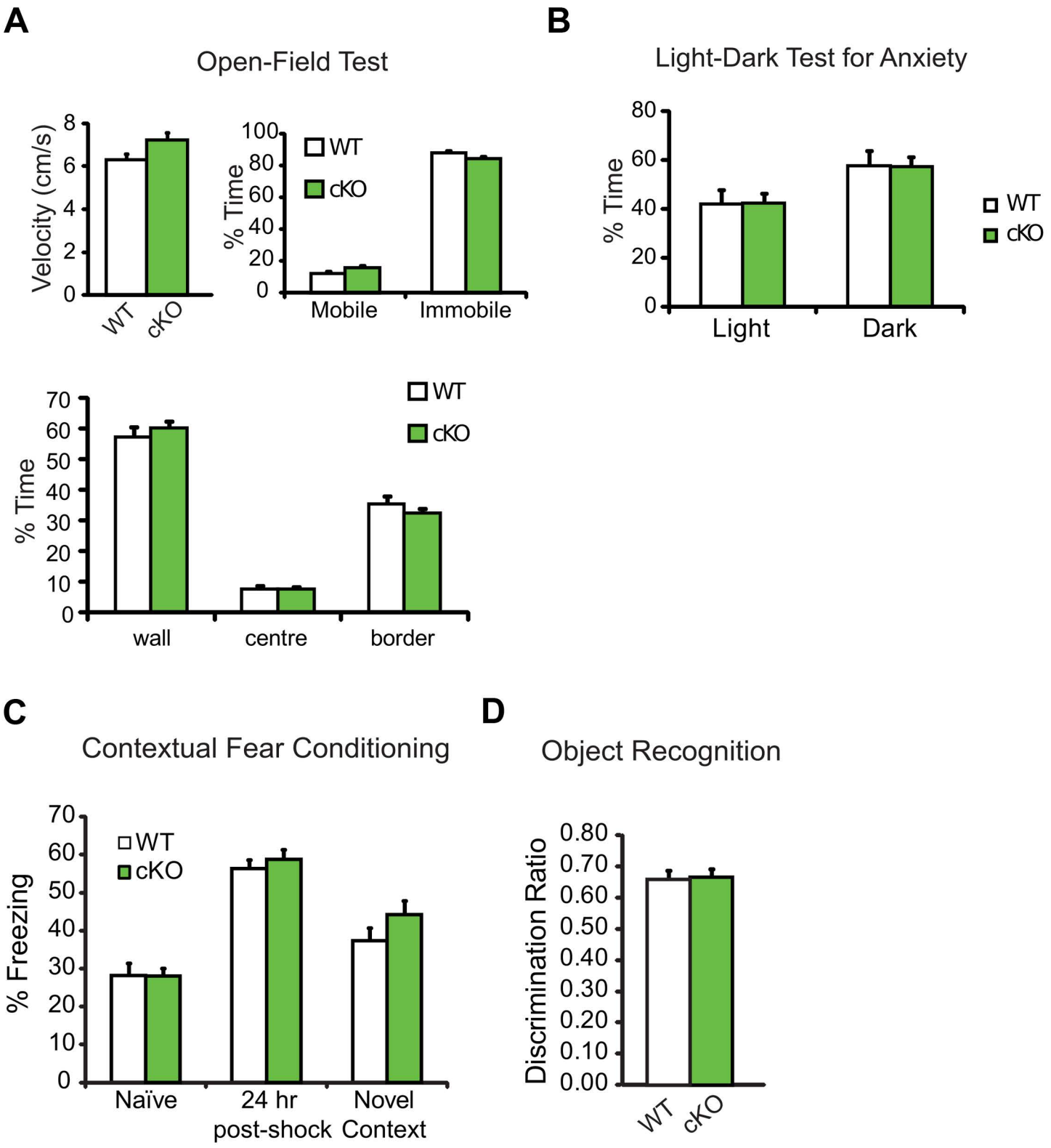
A
Open-Field Test
Velocity (cm/s)
WT
cKO
% Time
Mobile
Immobile
% Time
wall
centre
border
B
Light-Dark Test for Anxiety
% Time
Light
Dark
C
Contextual Fear Conditioning
% Freezing
Naïve
24 hr post-shock
Novel Context
D
Object Recognition
Discrimination Ratio

Figure S2

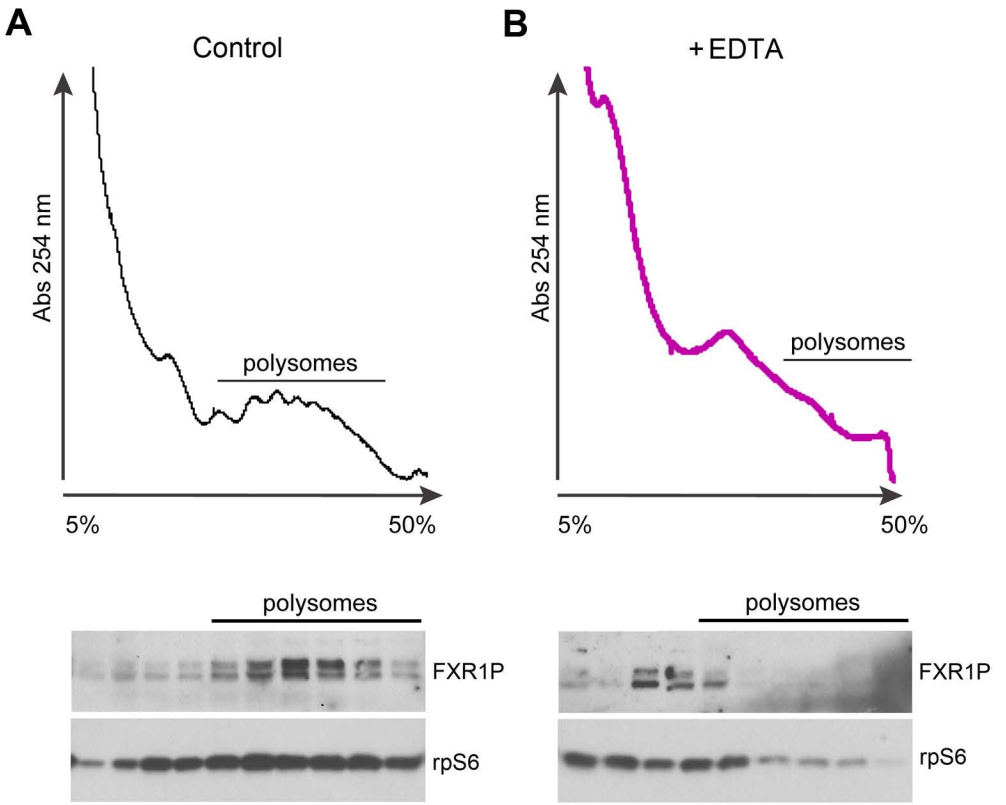
A
Control
Abs 254 nm
polysomes
5%
50%
B
+EDTA
Abs 254 nm
polysomes
5%
50%
polysomes
FXR1P
rpS6
polysomes
FXR1P
rpS6

Figure S3

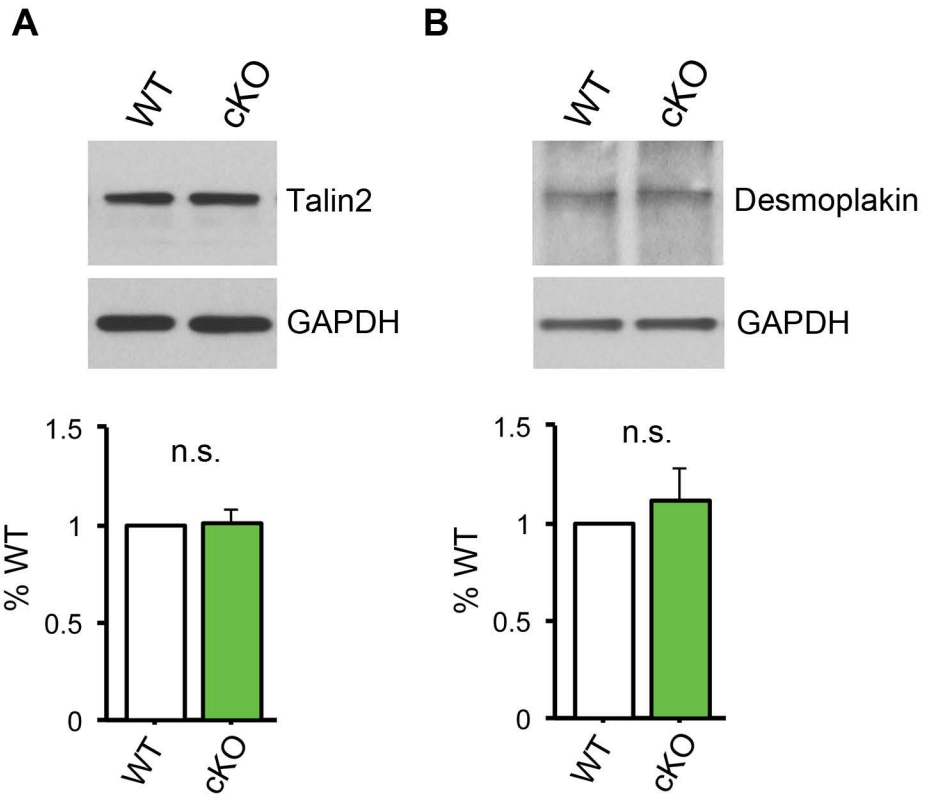
A
WT
cKO
Talin2
GAPDH
1.5
1
0.5
0
% WT
n.s.
WT
cKO
B
WT
cKO
Desmoplakin
GAPDH
1.5
1
0.5
0
% WT
n.s.
WT
cKO

Figure S4

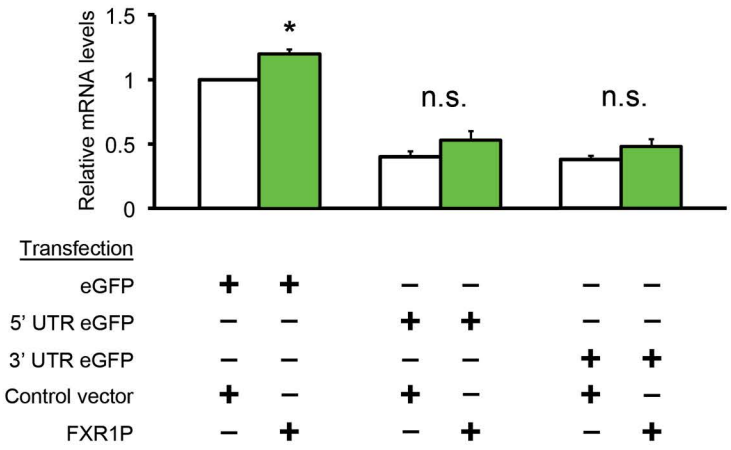
Relative mRNA levels
1.5
1
0.5
0
*
n.s.
n.s.
Transfection
eGFP + + – – – –
5' UTR eGFP – – + + – –
3' UTR eGFP – – – – + +
Control vector + – + – + –
FXR1P – + – + – +

Figure S5

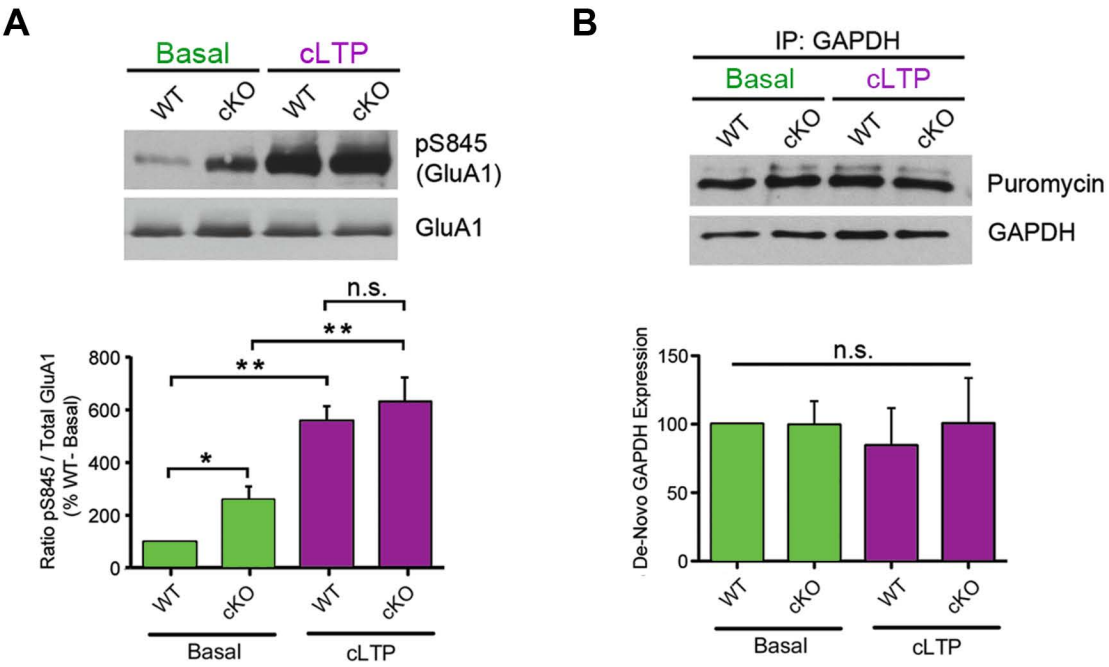
A
Basal
cLTP
WT
cKO
WT
cKO
pS845
(GluA1)
GluA1
n.s.
**
**
*
800
600
400
200
0
Ratio pS845 / Total GluA1
(% WT- Basal)
WT
cKO
WT
cKO
Basal
cLTP
B
IP: GAPDH
Basal
cLTP
WT
cKO
WT
cKO
Puromycin
GAPDH
n.s.
150
100
50
0
De-Novo GAPDH Expression
WT
cKO
WT
cKO
Basal
cLTP

Figure S6

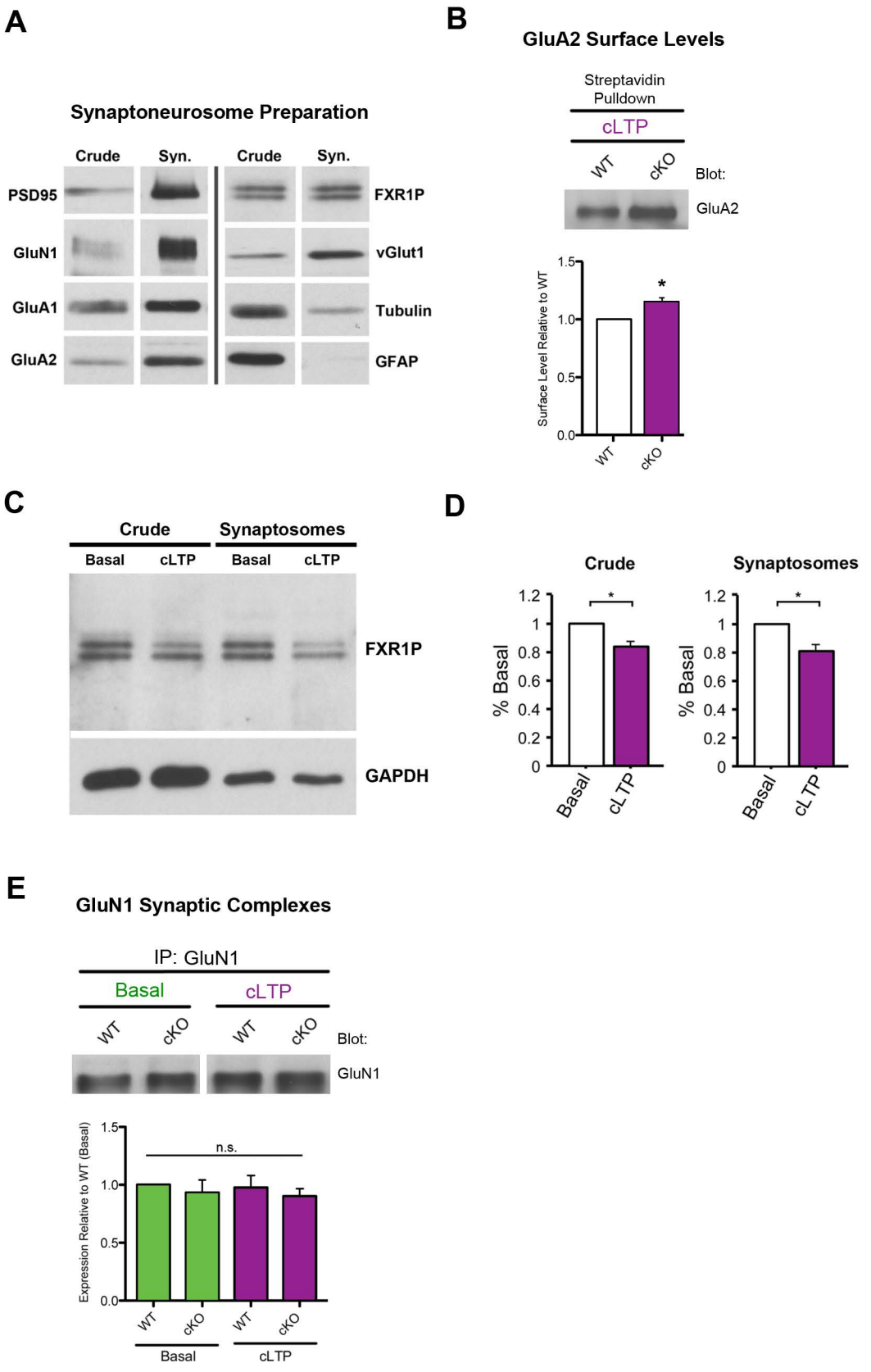
A
Synaptoneurosome Preparation
Crude
Syn.
Crude
Syn.
PSD95
FXR1P
GluN1
vGlut1
GluA1
Tubulin
GluA2
GFAP
B
GluA2 Surface Levels
Streptavidin Pulldown
cLTP
WT
cKO
Blot:
GluA2
Surface Level Relative to WT
1.5
1.0
0.5
0.0
*
WT
cKO
C
Crude
Synaptosomes
Basal
cLTP
Basal
cLTP
FXR1P
GAPDH
D
Crude
Synaptosomes
% Basal
1.2
1
0.8
0.6
0.4
0.2
0
*
*
Basal
cLTP
Basal
cLTP
E
GluN1 Synaptic Complexes
IP: GluN1
Basal
cLTP
WT
cKO
WT
cKO
Blot:
GluN1
Expression Relative to WT (Basal)
1.5
1.0
0.5
0.0
n.s.
WT
cKO
WT
cKO
Basal
cLTP

Figure S7

SUPPLEMENTAL FIGURE LEGENDS

Figure S1, related to Figure 1. Properties of the FXR1P cKO line. We crossed the αCaMKII-Cre (T29-1) driver line with a membrane-Tomato/membrane-GFP (mTomato/mGFP) reporter line in order to follow the pattern of Cre-recombination across postnatal development in the mouse hippocampus. **A.** *Left* Low magnification images of the hippocampus taken at different developmental time-points demonstrating the pattern of Cre-mediated recombination. Cells displaying recombination are marked by membrane-targeted green fluorescent protein (mGFP) expression. NeuN (magenta) staining delineates the cell body layers. Scale bar=100μm. *Right* High magnification view of the CA1 cell body layer showing the density of cells expressing mGFP. Scale bar=10μm. n=1 animal per time point. **B.** Representative low magnification images of MAP2, P0 and GFAP staining taken from the hippocampus of WT and FXR1P cKO mice. Loss of FXR1P did not lead to obvious differences in the levels or pattern of expression of MAP2, P0 and GFAP. Scale bar=100μm. *Insets* Higher magnification views of MAP2, P0 and GFAP staining. Scale bar=50μm. n=3 mice per genotype. **C.** Representative images of DiI-filled dendrites and dendritic spines taken from WT and FXR1P cKO mice. Scale bar=10μm. **D.** Loss of FXR1P caused a significant decrease (15%) in spine density on apical dendrites ($t(8) = 3.11$, $p=0.01$). **E-F.** Cumulative probability and bar plots showing the distributions and average spine lengths and spine head diameters from apical dendrites in WT and cKO mice (n = 8543 WT spines, n = 7635 cKO spines). Spine lengths on apical dendrites were reduced by 8% in the FXR1P cKO ($t(7) = 2.44$, $p=0.04$) (E). No change in average spine head diameter ($t(8) = -0.74$, $p = 0.48$) (F). **G.** Spines shapes were not altered in the FXR1P cKO (two-way mixed ANOVA, Genotype x Shapes, $F_{(2, 16)} = 1.91$, $p=0.18$). Dendrites were randomly selected for imaging from approximately 5 hippocampal slices per animal (~2 dendrites per slice, 10-15 dendrites/animal). n=5 WT mice from 5 litters, 66 dendrites and n=5 cKO mice from 5 litters, 69 dendrites (all male). All values represent means +/- standard errors. Unless otherwise stated, statistical analyses were performed using unpaired, two-tailed t-tests. *$p \leq 0.05$.

Figure S2, related to Figure 2. FXR1P cKO mice have normal motor and sensory behavior, general anxiety responses, and working memory. A. FXR1P cKO and WT mice performed similarly in all measures of the open field test (two-tailed, unpaired t-tests, $p>0.05$; n = 15 WT, n = 32 cKO). **B.** FXR1P cKO mice displayed normal anxiety responses in the light-dark box (two-tailed, unpaired t-tests, $p>0.05$; n = 16 WT, n = 32 cKO). **C.** FXR1P cKO and WT mice display similar freezing responses 24 hours after conditioning in both the shock context (two-way mixed ANOVA, Genotype x Pre/Post, $F_{(1,26)} = 0.42$, $p=0.52$) and a novel context (two-tailed, unpaired t-test, $p=0.17$; n = 15 WT , n =15 cKO mice, 8 litters, tested as 2 separate cohorts). **D.** Both WT and cKO mice spent similar amounts of time inspecting the novel object in a test of working memory (two-tailed, unpaired t-test, $p=0.84$; n=31 WT, n=34 cKO mice, 11 litters, tested as 4 separate cohorts), suggesting that cKO mice are not impaired in working memory. Discrimination Ratio = N/(N+F) where N = the duration for the novel object and F = the duration for the familiar object. All values represent means +/- standard errors.

Figure S3, related to Figure 4. FXR1P is associated with polyribosomes in adult mouse brain. A-B. Brain lysates were loaded onto 5% to 50% sucrose gradients and monosomes and polysomes separated by centrifugation. EDTA was included to disrupt polysomes and ensure that FXR1P co-sediments with translating ribosomes. Distribution of FXR1P and rpS6 (control) were monitored by Western blot.

Figure S4, related to Figure 4. Talin 2 and Desmoplakin are not altered in FXR1P cKO mice. A-B. Western blots showing that overall expression of Talin 2 and Desmoplakin are similar between adult WT and cKO mice (ps>0.05, two-tailed, one-sample t-test). GAPDH is used as a loading control. n.s. = not significant. Error bars show standard errors.

Figure S5, related to Figure 5. FXR1P does not change 5'UTR GluA2-eGFP or eGFP-3'UTR GluA2 mRNA levels. Bar graphs show average data for qRT-PCR experiments (relative to eGFP/Control vector condition) for each of the transfection combinations used. FXR1P-myc did not

affect the level of 5'UTR GluA2-eGFP nor eGFP-3'UTR GluA2 mRNA ($p>0.05$). However, a significant increase in eGFP mRNA was detected ($p=0.03$, two-tailed, one-sample t-test) upon co-transfection of FXR1P-myc in the eGFP condition. All values represent means +/- standard errors. n=3 separate cultures and transfections.

Figure S6, related to Figure 6. cLTP-dependent changes in WT and FXR1P cKO mice. A. cKO slices show increased basal phosphorylation of serine 845 (ratio of pS845 to total GluA1; $p\leq0.05$). Both WT and cKO slices showed increased serine 845 phosphorylation upon cLTP ($p\leq0.05$, two-tailed, unpaired two-sample t-test). **B.** Control experiments show that *de novo* synthesis of GAPDH is similar between genotypes under basal and cLTP conditions ($p>0.05$; n = 3 WT and 3 cKO mice). Unless otherwise stated statistical analyses were performed using two-tailed, one-sample t-tests. All values represent means +/- standard errors. n=4 WT and 4 cKO mice, unless otherwise stated. *$p\leq0.05$, **$p\leq0.01$, n.s. = not significant.

Figure S7, related to Figure 7. Synaptosome preparation from acute brain slices and following cLTP. A. Western blot analysis of crude lysates and synaptosomes from WT acute slices. Synaptosomes are enriched for synaptic molecules PSD95, GluN1, GluA1, GluA2, and vGlut1. FXR1P is also found in synaptosomes. Tubulin and GFAP are depleted in synaptosomes. **B.** Surface GluA2 is increased in cKO slices following cLTP ($p\leq0.05$; n=3 WT and 3 cKO mice). **C-D.** cLTP caused a reduction in overall (crude) and synaptosome-associated FXR1P ($p\leq0.05$; n=4 mice). GAPDH is a loading control. **E.** cKO slices show similar levels of GluN1 associated with GluN1 following immunoprecipitation from synaptosomes ($p>0.05$; n=3 WT and 3 cKO mice). Unless otherwise stated statistical analyses were performed using two-tailed, one-sample t-tests. All values represent means +/- standard errors. *$p\leq0.05$, n.s. = not significant.

EXTENDED EXPERIMENTAL PROCEDURES

DiI labeling of CA1 dendrites and imaging. Adult male mice (P60-P75) were transcardially perfused with 4% paraformaldehyde/0.1 M phosphate buffer; pH 7.4. The brain was post-fixed for 10 minutes and then transferred to PBS. The hippocampi were removed and cut into 300 μm slices using a tissue chopper. CA1 cells were labelled using the lipophilic fluorescent dye, DiI (Molecular Probes) (Gan et al., 2000). All manipulations were performed blind to animal genotype. CA1 dendrites were imaged using a 60X, 1.25 NA objective mounted on an Ultraview spinning disk confocal system. The primary apical dendrites of CA1 pyramidal cells (~ 100 μm from the cell body) were imaged. Z-stacks were produced using a z-step of 0.3 μm. The automated 3D analysis software NeuronStudio was used to compare spine parameters in WT and cKO mice.

Antibodies used for immunofluorescence. Rabbit anti-FXR1P (#ML13, 1:5000) (Cook et al., 2011), rabbit anti-MAP2 (Millipore, 1:1000), mouse anti-GFAP (Sigma, 1:1000), human anti-ribosomal P antibodies (Immunovision, 1:5000), mouse anti-NeuN (Millipore, 1:5000) and rabbit anti-GFP (Invitrogen, 1:1000).

Antibodies for Western blotting. Antibodies used: rabbit anti-FXR1P #ML13 (1:50,000-1:100,000), rabbit anti-pan CaMKII (Cell Signaling Technology; 1:900), mouse anti-FXR2P clone A42 (Millipore; 1:2000), mouse anti-FMRP clone 1C3 (Millipore; 1:2000), mouse anti-vGlut1 clone N28/9 (Neuromab; 1:7000), mouse anti-PSD95 clone K28/43 (Neuromab; 1:500,000), mouse anti-PKMzeta clone H-1 (Santa Cruz; 1:2000), mouse anti-AGO2 (Abnova; 1:3000), mouse anti-eIF4E (R&D Systems; 1:6000), mouse anti-GluA1 (Millipore; 1:9000), mouse anti-GluA2 clone 6C4 (Millipore; 1:3000), rabbit anti-GluA1 (Millipore; 1:3000), mouse anti-GluA2 (Neuromab; 1:2000), mouse anti GluN1 (BD Phamingen; 1:7000), rabbit anti-phospho GluA1 Ser-845 (Millipore; 1:5,000), anti-Talin 2 (Abcam; 1:10,000), anti-desmoplakin (Millipore; 1:2000), anti-rpS6 (Santa Cruz: 1:5000), and mouse anti-puromycin (KeraFAST; 1:4-5,000). Mouse anti-GAPDH (Abcam; 1:10,000) or mouse anti-GAPDH

clone 6C5 (Millipore; 1:300,000) was used as a loading control for all blots.

GluA2 reporter assays and FXR1P binding to the GluA2 5'UTR. HEK 293T cells were maintained in Dulbecco's modified Eagle's medium (DMEM) supplemented with 10% (v/v) FBS (fetal bovine serum) (Invitrogen) and 1% (v/v) penicillin/streptomycin (Invitrogen). Cells were transfected in 6-well plates using Lipofectamine 2000 (Invitrogen) according to the manufacturer's instructions. 0.5 μg of eGFP-N3, GluA2 5'UTR-eGFP, GluA2 3'UTR-eGFP (La Via et al., 2013) or Δ5'UTR GluA2 were cotransfected with 2 μg of pcDNA3, FXR1P-Myc, FXR2P-Myc or FMRP-Myc as specified in Figure 5. At 6 hours post-transfection, the media was replaced with plain DMEM and cells were serum-starved for a further 18 hours (Vasudevan and Steitz, 2007). Cell lysates were prepared using RIPA buffer (1% Triton X-100, 1% sodium deoxycholate, 0.1% SDS, 20 mM Tris pH 8.0, 150 mM NaCl and 1 mM EDTA, and protease inhibitors) and eGFP expression was assessed by Western blotting (mouse anti-GFP clone JL-8, 1:10,000; Clontech). Expression of Myc constructs were detected using a mouse anti-Myc antibody clone 9B11 (Cell Signaling; 1:10,000). For mRNA analysis, RNA was extracted using RNeasy Plus Mini Kit (Qiagen) and reverse transcription and quantitative real-time PCR were performed as described above. The following primer sequences were used: hGAPDH forward, AATCCCATCACCATCTTCCAG; hGAPDH reverse, AAATGAGCCCCAGCCTTC; eGFP forward, GACGGCAACTACAAGACCCG; eGFP reverse, CTCCTTGAAGTCGATGCCCT. To assess binding of FXR1P to GluA2 5'UTR, we synthesized biotinylated RNA probes containing either the 5'UTR GluA2 or Δ5'UTR GluA2 sequences using Biotin-11-CTP (Enzo Life Sciences) and a MEGAscript kit according to the manufacturer's instructions (Ambion). Biotinylation levels were verified by dot blot using Streptavidin HRP (GE Healthcare; 1:15,000) (Figure 5). Serum-starved HEK 293T cells expressing FXR1P-Myc (as described above) were lysed in RNA binding buffer (20 mM Tris (pH 7.5), 150 mM NaCl, 1 mM EDTA, 1 mM EGTA, 1% (v/v) Triton X-100 supplemented with protease inhibitors). Cell lysates were incubated with 20 nmoles of biotinylated RNA in the presence of 2 mg/ml

Heparin and RNaseOUT (Invitrogen, 100U/ml) for 1 hour at 4ºC on a rotating platform. 50 µl of equilibrated Streptavidin-sepharose (Sigma) beads were added for a further 30 minutes. Beads were washed 3X with RNA binding buffer and complexes were eluted with 3X sample buffer, then subjected to SDS-PAGE and Western blotting for Myc (as above).

Behavioral Paradigms.

Open field test. Mice were placed in the center of a transparent open field testing chamber (50 cm x 50 cm x 45 cm) and allowed to freely explore the chamber for a total of 10 minutes. All measurements were generated using Ethovision (Noldus, Attleboro, MA).

Dark–light box test. Mice were placed in the middle of the brightly lit chamber (60 W light bulb) facing away from the partition dividing the brightly lit chamber (29 cm x 20.4 cm x 22 cm) from the dark chamber (15.5 cm x 20.4 cm x 22 cm). Mice were allowed to freely explore and transition between the two chambers for a total of 10 minutes. The total time spent in the dark and light partitions were manually recorded.

Contextual fear conditioning. Contextual fear conditioning was conducted in three identical chambers, measuring 26 x 20 x 20 cm, with steel-grid floors. Photocells located along the periphery of the chambers recorded the animal's location and movements. Conditioning (day 1) was performed using two shocks (0.5 mA, 2 secs) separated by 2 minutes. The amount of time spent freezing was recorded by an automated system (Accuscan, Columbus, OH). On day 2, animals were placed into the chambers for 5 minutes, without shock, and freezing was recorded. On day 3, animals were placed into a novel context and freezing was recorded for 5 minutes (without shock delivery).

Object recognition test. This test was conducted in an arena constructed of grey, opaque Plexiglas measuring 44.5 x 44.5 x 49.5 cm, located in a sound-attenuating room illuminated by 2 60 W red light bulbs. On day 1, animals were individually placed into the arena for 10 minutes without any objects, to habituate to the arena. On day 2, two pyramids were placed along a diagonal of the open field, offset 10

cm from the corners. Animals were placed into the arena and allowed to freely explore for 10 minutes. They were then returned to their holding cages for 10 minutes, and then placed back into the area which contained one pyramid (the familiar object) and one plastic hen (the novel object) for 5 minutes. The positions of the novel and familiar objects were counterbalanced across animals. All trials were recorded to DVD with an infrared camera and these videos were then analyzed with the Top Scan 2.0 tracking system (CleverSys, Virginia, USA). Exploration was defined as the time in which the animal's nose was within 1 cm of the object.

Modified Morris water maze task. The maze consisted of a 1.2 m diameter circular pool filled (45 cm depth) with water (22° C) made opaque with white liquid Gouache. A 10 cm^2 platform submerged 2 cm below the surface of the water was placed in the center of one quadrant of the pool. All measures were automatically recorded using the HVS 2100 tracking system (HVS, Buckingham, UK).

The first phase of the experiment, standard training, consisted of three trials per day for five days. The platform was located in the south-west quadrant of the pool. Animals that found the platform within 60 sec were allowed to remain on the platform for 30 sec; those that did not were manually placed on the platform for the same time period. Four hours after the third trial of day 5, a 60 second probe test, in which the platform was removed from the pool, was conducted. For standard training: n=28 WT, n=28 cKO mice, 15 litters, tested in 3 separate cohorts.

Following a nine day rest period, the second phase of the experiment, designated retraining, was conducted. This phase consisted of three trials per day over four consecutive days.

Following a two day rest period, the final phase of the experiment, reversal training, was conducted. During the first trial of reversal training day 1, the platform was also located in the south-west quadrant, however, on the second and third trials the platform was moved to the opposite (north-east) quadrant. Subsequent reversal training consisted of three trials per day for five consecutive days with the platform located in the north-east quadrant. Four hours after the third trial of the last day of reversal training, a 60 second probe test, in which the platform was removed from the pool, was

conducted. Animals were released into the south-west quadrant. For retraining and reversal training: n=20 WT, n=20 cKO mice, 11 litters, tested in 2 separate cohorts.

qRT-PCR. Total RNA was extracted from whole hippocampi or cerebellum of adult mice (8-12 weeks) using RNeasy Lipid Tissue (Qiagen) and first strand synthesis was performed with Quantitech RT-PCR Kit (Qiagen) primed with random primers. Quantitative real-time PCR was performed in a StepOne Plus Thermocycler (ABI) with Fast SYBR Green Master Mix. mRNA levels were quantified using the ddCT method of quantification with GAPDH as the internal control. The following primer sequences were used: Mouse GAPDH, Forward ATGTGTCCGTCGTGGATC, Reverse TTGAAGTCGCAGGAGACAACC; FXR1P, Forward CGAAGACTCCCTCACAGTTG, Reverse ACCTCTACTTCATCTCCTTCACT; GluA2, Forward AAAGAATACCCTGGAGCACAC, Reverse CCAAACAATCTCCTGCATTTCC; GluN1, Forward CGGAGCACACTGGACTCATT, Reverse ATCGGCCAAAGGGACTGAAG.

SUPPLEMENTAL REFERENCES

Cook, D., Sanchez-Carbente, M. del R., Lachance, C., Radzioch, D., Tremblay, S., Khandjian, E.W., DesGroseillers, L., and Murai, K.K. (2011). Fragile X related protein 1 clusters with ribosomes and messenger RNAs at a subset of dendritic spines in the mouse hippocampus. PLoS One *6*, e26120.

Gan, W.B., Grutzendler, J., Wong, W.T., Wong, R.O.L., and Lichtman, J.W. (2000). Multicolor "DiOlistic" labeling of the nervous system using lipophilic dye combinations. Neuron *27*, 219–225.

Vasudevan, S., and Steitz, J.A. (2007). AU-rich-element-mediated upregulation of translation by FXR1 and Argonaute 2. Cell *128*, 1105–1118.

La Via, L., Bonini, D., Russo, I., Orlandi, C., Barlati, S., and Barbon, A. (2013). Modulation of dendritic AMPA receptor mRNA trafficking by RNA splicing and editing. Nucleic Acids Res. *41*, 617–631.